

DOI: [10.5281/zenodo.17142884](https://doi.org/10.5281/zenodo.17142884)



Nonlinear Performance Evaluation of Reinforced Concrete Frames with Off-axis Steel Braces

Yousef Shiri

PhD in Civil Engineering, Structural Engineering, Kharazmi University

*Corresponding author: yousefshiri1978@gmail.com

Published: 18 September 2025

Accepted: 09 September 2025

Received: 03 August 2025

Abstract: In recent years, the use of steel bracing in reinforced concrete structures has been proposed for the purpose of strengthening existing weak buildings and also in the seismic design of new buildings as a shear-resistant element against earthquakes. The use of steel bracing with direct connection has been considered for several reasons, including economic issues, easy implementation, and the possibility of securing and strengthening weak reinforced concrete structures against earthquakes. One of the metal bracings used is the Sherwin divergent bracing, which, due to its very suitable and balanced performance, both increases the stiffness and reduces the maximum displacements of the structure, and by absorbing more energy in nonlinear ranges, increases the ductility and, as a result, increases the behavior coefficient of the structure and improves its performance when entering the inelastic range. In this study, the performance behavior of a reinforced concrete structure in two cases, first: a code-accepted design and second: a weakness in the code design, which is strengthened by an off-axis steel bracing, is investigated using nonlinear Pushover analysis and the results of different forms of changing the bracing bond length and its effect on the performance of the strengthened structure are compared. The results show an improvement in performance in the field of linear behavior by increasing stiffness and reducing P- Δ effects, which is one of the main weaknesses in reinforced concrete structures due to the formation of cracks, and in the field of nonlinear behavior against severe earthquakes, a significant increase in capacity and a reduction in ductility requirements in the reinforced concrete flexural frame structure strengthened with a divergent steel bracing.

Keywords: Reinforced concrete frame, steel divergent brace, strengthening, nonlinear performance, pushover, ductility

1- Introduction

According to the following equation, which is known as the dynamic equilibrium equation of structures, it can be easily seen that if, for example, the damping (C) of the structure increases, in order to maintain the dynamic equilibrium of the structure and assuming that the input force to the structure is known, the displacement and acceleration of the structure must be reduced.

$$M\ddot{U} + C\dot{U} + KU = P(t)$$

In the above equation, M represents the mass of the structure, C is the damping of the structure, K is the stiffness of the structure, U is the displacement of the structure, \dot{U} is the velocity of the structure, and $p(t)$ is the dynamic force acting on the structure.

Increasing the damping reduces the displacement or displacement and the shear force applied to the structure. Pure stiffness can be created by means such as braces. With increasing stiffness, the displacements in the structure are reduced but the shear force applied to the structure increases.[6 ,5 ,4 ,3 ,2 ,1]

Although the subject of reinforced concrete frames braced with steel braces is relatively new, a relatively large amount of research has been conducted on this subject. Research conducted in this field has mainly focused on the behavior of convergent braces, which have investigated the stiffness and strength of the system. However, the aim of this research is to investigate the nonlinear behavior, ductility, and failure modes of the system strengthened with divergent braces. This research can be used to retrofit inefficient or already damaged concrete structures after the desired results are achieved.

Perhaps the first application of this system was in the retrofitting of schools in Japan. This building, which had short columns, suffered heavy damage to the columns in a severe earthquake in 1978 and was retrofitted with steel perimeter bracing [7]. The second case was the use of this method in 1980, in a twelve-story building in Mexico City, where the concrete building was retrofitted with rigid perimeter frames and steel perimeter bracing and showed good seismic behavior in a severe earthquake in 1985 [8]. The third case was in a hospital, also in Mexico City, which was retrofitted after the 1985 earthquake. In this building, unlike the previous two cases, steel braces were placed inside the openings of the perimeter frames, and in subsequent earthquakes it was shown that the brace acts as a member of the frame. In parallel with these applications, in the first research conducted in this case, which was carried out in the 1980s, only the possibility of using this strengthening method to increase the lateral resistance of concrete frames was mentioned and the effectiveness of this method was confirmed [8]. In 1990, Badoux and Jirsabangahi investigated the behavior of braced concrete frames under lateral loads, especially cyclic loads. In this study, the effect of brace slenderness on the amount of energy absorbed by the frame was considered and it was shown that the

inelastic buckling of the compression brace is an important factor in reducing the amount of energy absorbed [9]. Various studies have been conducted on this subject from 1990 to 1995, some of which have emphasized the effectiveness of this strengthening method in increasing lateral strength and ductility, and in some cases, the economic efficiency of the method has been proven. Some researchers have investigated the connections of braces to frames, and it has been found that the use of root reinforcements for the connection plate, which are placed in the concrete frame with the help of a Hilti, and the use of epoxy adhesive to connect the connection plate, are effective methods for designing these connections. In addition, it has been found that limited reinforcement of the beam-column and brace connections will improve the behavior of the frame. Several researchers have also conducted studies on the behavior of braces with dampers and post-tensioned braces, and have confirmed the effectiveness of these methods in strengthening concrete frames [10]. In 1995, Maheri and Sahibi reported an experimental study on concrete frames with cross braces, single tension braces, and single compression braces, and showed that although steel materials behave similarly in tension and compression, tension braces contribute more to the shear capacity of the frame than compression braces. It was also shown that when cross braces are used, the shear capacity of the frame is about 1.5 times that of single tension and compression braces [11]. In 2001, Gobara and Boualfas modeled the inelastic behavior of a reinforced concrete structure with two options: cross braces and inverted V divergent braces with shear connections at the ends of the braces in the DRAIN software and showed that under the influence of twelve different significant earthquakes, the divergently braced frame has a reliable non-brittle behavior [8]. Khatib et al. (1988) conducted a comprehensive study on the pre-buckling and post-buckling behavior of figure eight braces. Normally, the compressive deflection of braces is less than their tensile deflection, and this causes a very large asymmetric shear force on the center of the beam during earthquake force cycles after buckling. In this study, Khatib suggested that this force be transferred to the upper floors by placing a zipper element at the vertices of the braces. To prevent the gravity load from entering, this element is not present on the first floor. If the compression brace on the first floor buckles while the other braces are in the elastic range, an unbalanced vertical force is created in the middle of the first floor beam span. The unbalanced force transmitted by the zipper element increases the compressive force on the second-story compression brace, eventually causing that brace to buckle as well. If the applied force continues to move the frame in the same initial direction, a large unbalanced force is distributed throughout the structure, until the remaining compression braces also buckle.[12]

In this study, after validation using Etabs2015 software, reinforced concrete frame models were created in two cases; a concrete frame designed in accordance with Code 2800 and ACI318-08 and a case where the design was done with weakness, in different shapes of off-axis Sherwin bracing with variable beam lengths, in the software and their results were extracted and after comparing them, the most optimal retrofitted case was introduced ,[13] .[18 ,17 ,16 ,15 ,14

-2 Validation

Modeling was done using Etabs2015 software. In order to validate the results of the simulation with this software, the tested frame was first examined by researchers at the University of Tokyo. This concrete frame was tested by Vekiwo and Amara (1992) under the effect of increasing static load. Therefore, this frame is modeled in the software and its results are compared with the results of the experiment.

-1-2 Specifications of the Vekivu and Amara test specimen

The aforementioned laboratory program, including the loading method, the location of the displacement measurement sensors, etc., is shown in Figure 1.

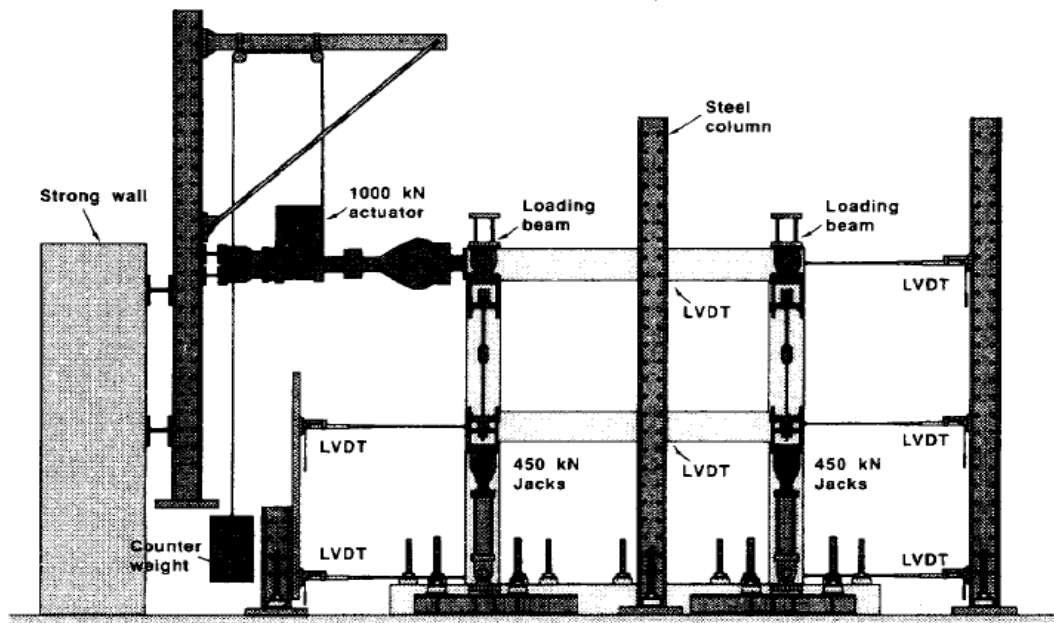


Figure 1 – Test setup of the Vekiwo and Amara (1992) experiment

The geometric specifications of the reinforced concrete frame, including the span length, story height, cross-section dimensions, and beam and column cross-section reinforcements, are also presented in Figure 2.

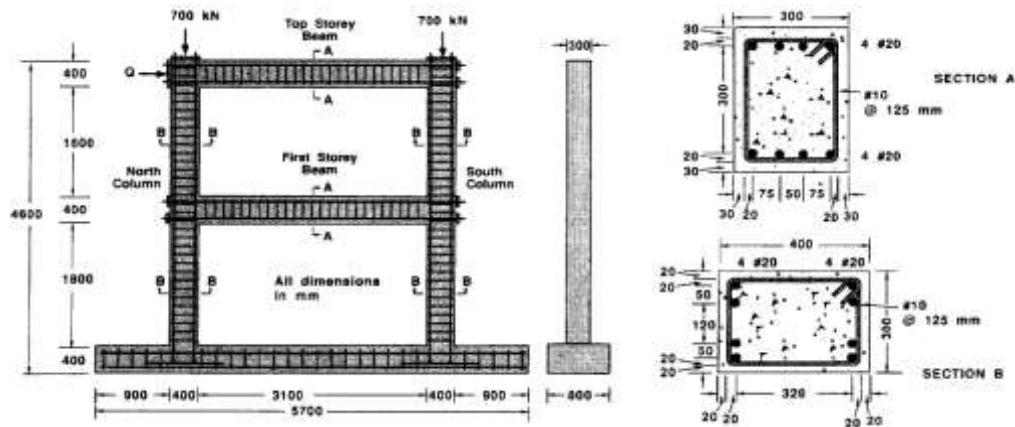


Figure 2 – Characteristics of the reinforced concrete frame by Kivu and Amara (1992)

As shown in the figure above, the longitudinal reinforcement of the section is 20 bar and the transverse reinforcement is of the closed yoke type (10 bar) which is placed at intervals of 125 mm along the length of the member.

The aforementioned concrete frame is made of concrete with a compressive strength of 30 MPa. The yield stress of the 20 bar reinforcement is reported to be 400 MPa and the yield stress of the 10 bar reinforcement is reported to be 440 MPa. The stress-strain curve of the concrete resulting from the control displacement test is shown in Figure 3 and the behavior curve of the reinforcement is shown in Figure 4.

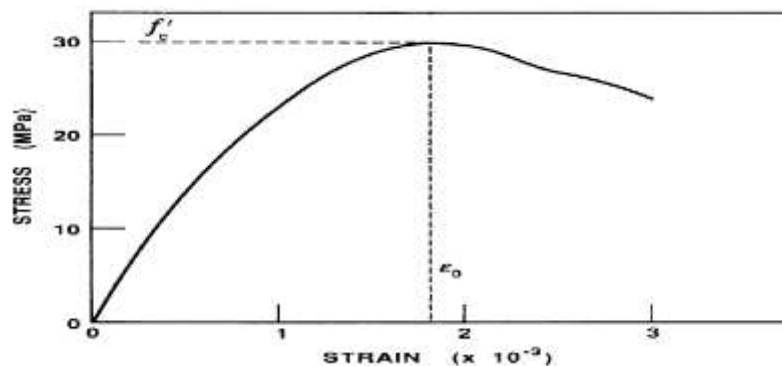


Figure 3 – Concrete compressive behavior curve

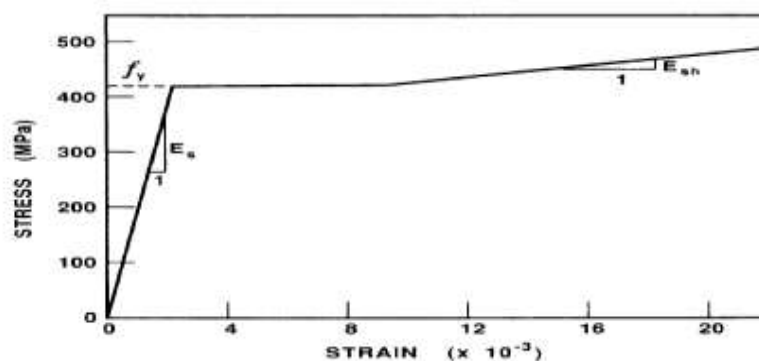


Figure 4 – Rebar behavior curve

As shown in Figure 1, a 70-ton gravity load is applied to each column during the test, and an increasing lateral load is applied at the second floor level. Therefore, the roof force-displacement response is selected as the known parameter of the test and the unknown parameter of the modeling.

2-2- Modeling

The modeling was performed in the finite element software Etabs2015. In order to determine the response of the aforementioned frame, a static pushover analysis must be performed. The following steps are shown in the analysis. First, according to Figure 5, the initial model of the structure is built in the software and boundary conditions and gravity loads are applied to it. Then, the elastic properties of the concrete and rebars are defined in the software based on the data obtained from the Vekiwo and Amara test, and the beam and column sections are also defined. In the next step, the nonlinear behavior of the reinforced concrete frame members must be considered. In order to perform nonlinear material analysis, there are various methods, one of the most practical methods is the focused plasticity method, in other words, the step-by-step plastic analysis. In this method, the entire nonlinear behavior of a member, in the place where it experiences the most plastic deformations, is considered centrally by considering a plastic joint. The characteristics of the joints are defined in terms of cross-sectional dimensions, reinforcement amount, axial load, shear force and material characteristics. ASCE41-13 publication has been used to define the joints. Therefore, beams are assigned a flexural joint and columns are assigned an axial load-flexural moment interaction joint (using fiber elements).

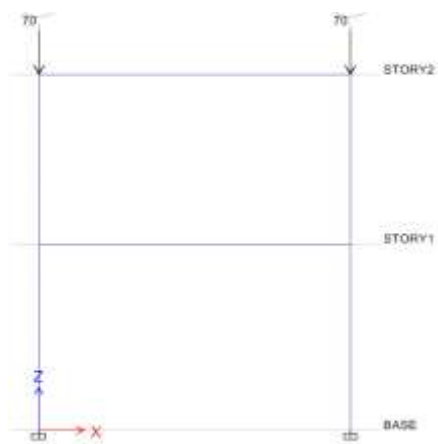


Figure 5 - Model built in the software

After defining the nonlinear characteristics of the members, it is necessary to introduce pushover analysis to the software. For this purpose, a nonlinear solution for the gravity load is first defined as Gravity and after applying it to the structure, its applied effects are used as the boundary conditions of the pushover analysis. The lateral nonlinear analysis was performed according to the experiment using a lateral load at the roof level. The state of the

structure during the formation of the mechanism, in other words, at the collapse stage, is seen in Figure 6 and it is clear that in the collapse stage of the mechanism, the bending joints of the beams along with the column foot joints caused the collapse of the structure, which is consistent with the test report.

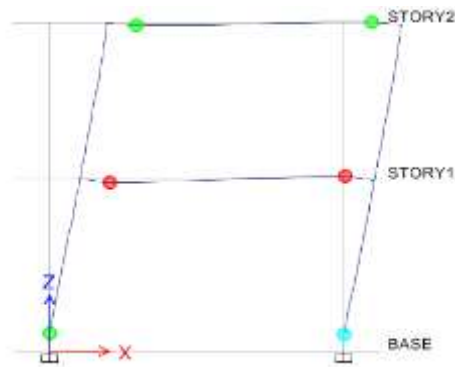


Figure 6 – Formation of the mechanism during collapse in the structure

The response of the concrete frame is shown in Figure 7. In this figure, the lateral load applied to the roof level is shown relative to the roof displacement, which can be seen from the experimental values showing a relatively good agreement with the numerical model.

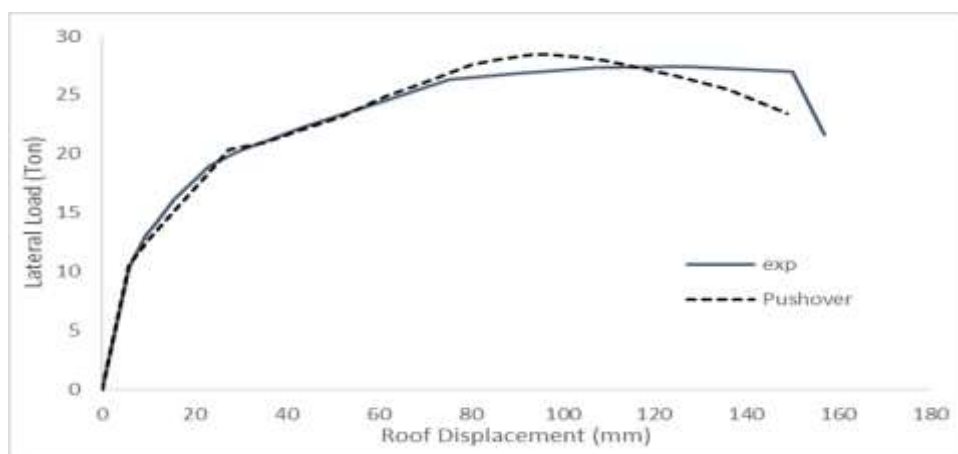


Figure 7 - Comparison of experimental and numerical response of the structure

-3Reinforcement of concrete frame using divergent steel brace

In this section, the reinforcement of a reinforced concrete frame with a flexural frame system is carried out by adding divergent steel braces. For this purpose, two cases are considered. In the first case, a structure that has been designed and implemented using seismic design codes is examined. However, in the second case, a structure is examined whose design is extremely problematic and, in other words, collapses in the design earthquake. ETABS2015 software has been used in all modeling, which was validated in the previous section.

-1-3Characteristics of the base structure

The base structure in this study is a two-dimensional reinforced concrete frame that has three spans on three floors. The spans are 5 meters long and the floors are 4 meters high. The geometry of the desired frame is shown in Figure 1.

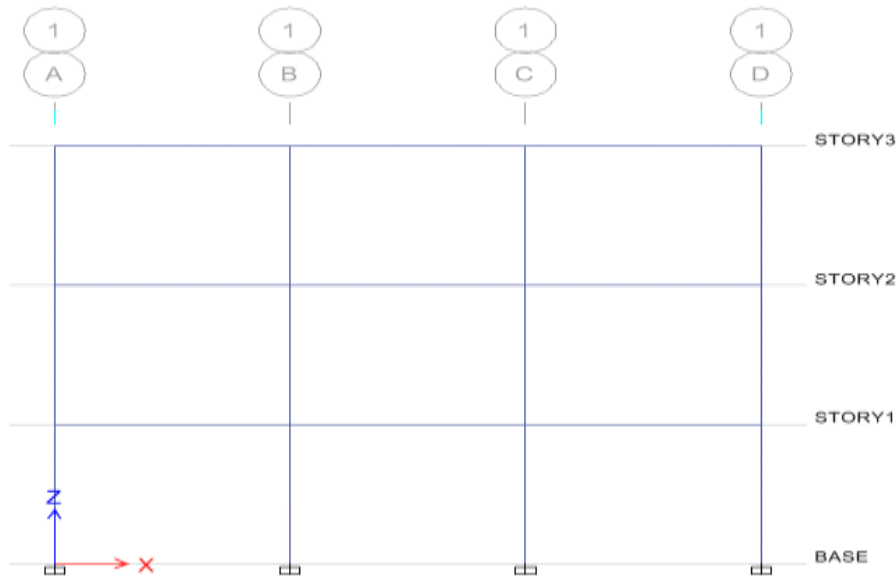


Figure 8- Concrete flexural frame geometry (base structure)

The material specifications in all models are as follows: C30 grade concrete with a compressive strength of 30 MPa and S400 rebar with a yield stress of 400 MPa have been used.

-1-1-3First case

The structure shown in Figure 8 is first designed using Code 2800 and ACI318-08 and then evaluated using a nonlinear static method. It should be noted that the performance level of the structure is evaluated using the criteria of Publication 360 of the Presidential Strategic Planning and Supervision Office and also the ASCE41-13 Code. In the initial design, the structural system is considered to be a reinforced concrete flexural frame with medium ductility. Therefore, the earthquake coefficient is calculated as 0.154, which after designing the structure, the cross-section of the beams of all floors is square with dimensions of 40 cm and the upper and lower reinforcements are $5\phi 20$ and $3\phi 20$, respectively. Also, the dimensions of the columns of the ground floor are 50 cm and the dimensions of the columns of the higher floors are 40 cm. It is necessary to explain that the longitudinal reinforcements of the column sections are $\phi 25$ and its transverse reinforcements are $\phi 10@125$ mm. The designed structure is evaluated using the nonlinear static method and based on the modeling, analysis and acceptance criteria of the 360 publication. In order to define the plastic joint model of the beams, Table 6-8 of the 360 publication, shown in Figure 9, is used.

| معیارهای پذیرش ^{۸ و ۹} | | | | پارامترهای مدل‌سازی ^۱ | | | شرایط | | | |
|--|--------|--------|--------|----------------------------------|--------------------------------|--------|--|---------------------------|--------------------------|-------|
| زاویه‌ی دوران خمیری، رادیان | | | | نسبت مقاومت باقیمانده | زاویه‌ی دوران خمیری، رادیان | | | | | |
| سطح عملکرد | | | | | | | | | | |
| نوع عضو | | | | | | | | | | |
| غیر اصلی | | اصلی | | | | | | | | |
| CP | LS | CP | LS | | | | | | | |
| IO | | | | c | b | a | | | | |
| الف = تیرهایی که با خمش کنترل می‌شوند ^{۸ و ۹} | | | | | | | | | | |
| | | | | | | | $\frac{2F_v}{V_{ps}} \leq \frac{I_c}{I_c}$ | آرماتور عرضی ^۴ | $\frac{p - p'}{p_{bal}}$ | |
| -/۰.۵ | -/۰.۲ | -/۰.۲۵ | -/۰.۲ | -/۰.۱۰ | -/۲ | -/۰.۵ | -/۰.۲۵ | ≤ ۳ | C | ≤ ۰/۰ |
| -/۰.۴ | -/۰.۲ | -/۰.۲ | -/۰.۱ | -/۰.۰۵ | -/۲ | -/۰.۴ | -/۰.۲ | ≥ ۶ | C | ≤ ۰/۰ |
| -/۰.۳ | -/۰.۲ | -/۰.۲ | -/۰.۱ | -/۰.۰۵ | -/۲ | -/۰.۳ | -/۰.۲ | ≤ ۳ | C | ≥ ۰/۵ |
| -/۰.۲ | -/۰.۱۵ | -/۰.۱۵ | -/۰.۰۵ | -/۰.۰۵ | -/۲ | -/۰.۲ | -/۰.۱۵ | ≥ ۶ | C | ≥ ۰/۵ |
| -/۰.۳ | -/۰.۲ | -/۰.۲ | -/۰.۱ | -/۰.۰۵ | -/۲ | -/۰.۳ | -/۰.۲ | ≤ ۳ | NC | ≤ ۰/۰ |
| -/۰.۱۵ | -/۰.۱ | -/۰.۱ | -/۰.۰۵ | -/۰.۰۵ | -/۲ | -/۰.۱۵ | -/۰.۱ | ≥ ۶ | NC | ≥ ۰/۰ |
| -/۰.۱۵ | -/۰.۱ | -/۰.۱ | -/۰.۱ | -/۰.۰۵ | -/۲ | -/۰.۱۵ | -/۰.۱ | ≤ ۳ | NC | ≥ ۰/۵ |
| -/۰.۱ | -/۰.۰۵ | -/۰.۰۵ | -/۰.۰۵ | -/۰.۰۵ | -/۲ | -/۰.۱ | -/۰.۰۵ | ≥ ۶ | NC | ≥ ۰/۵ |

Figure 9- Table 6-8 of the 360 publication

According to the amount of beam reinforcement and its bracing method, the first row of the above table is used. It should be noted that in the design of the base structure, all the criteria of the 2800 Code and the ninth topic of the National Building Regulations have been observed, therefore, the condition of the beams in terms of bracing is qualified for condition C in the above table and the existing shear value also meets the conditions of the first row. On the other hand, to define the plastic joint model, it is necessary to introduce the yield moment value in the beam section for both positive and negative anchors to the software. The upper and lower reinforcements of the section are $5\phi 20$ and $3\phi 20$, respectively. Therefore, the positive yield moment is equal to 18 ton.m and the yield moment is equal to 27 ton.m. According to the above explanations, the plastic joint behavior model of beams is defined in ETABS 2015 software and using this model, two joints are defined at the beginning and end of all beams. However, in order to define the plastic joint model in columns, the Fiber P-M2-M3 joint is defined. For this purpose, the entire cross-section is modeled using fiber elements. The location of the joints assigned to beams and columns is presented in Figure 10.

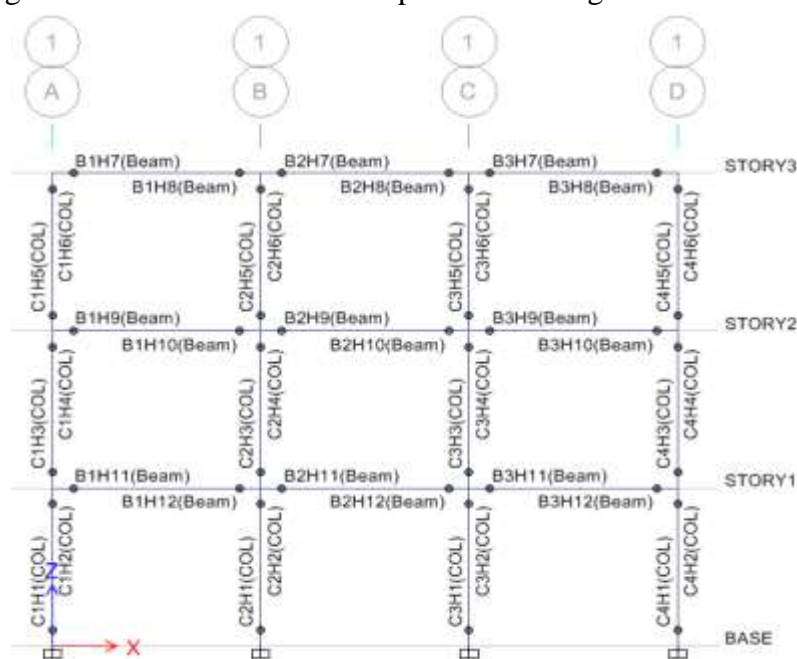


Figure 10 - Location of plastic joints in beams and columns Another issue in defining fiber plastic joints is that the behavior of concrete and steel must also be introduced into the software in a nonlinear manner. The nonlinear behavior of concrete is considered according to Figure 11 and the nonlinear behavior of reinforcement is considered according to Figure 12.

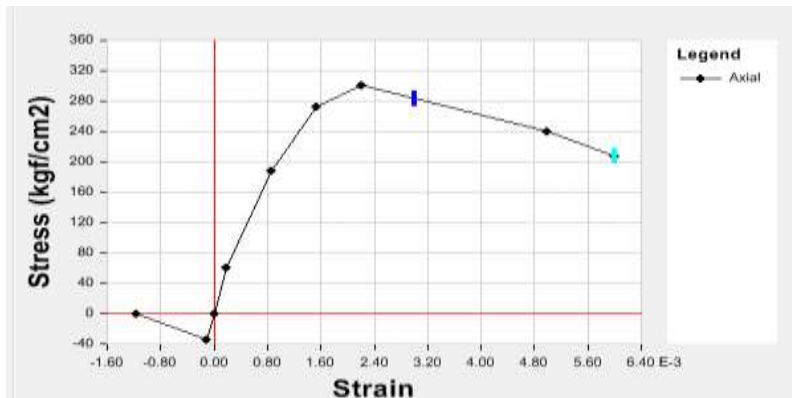


Figure 11 - Concrete stress-strain curve

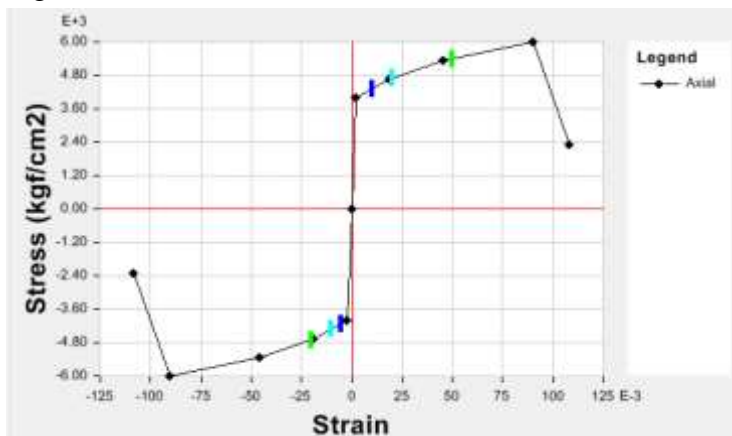


Figure 12 - Reinforcement Stress-Strain Curve

After defining the nonlinear behavior of the structure, gravity loads are first applied to the structure, followed by incremental lateral loads. According to the new edition of the 360 publication, the lateral load distribution used in nonlinear static analysis is considered to be proportional to the first mode of the structure. The capacity curve of the structure, which shows the base shear versus roof displacement, is shown in Figure 13.

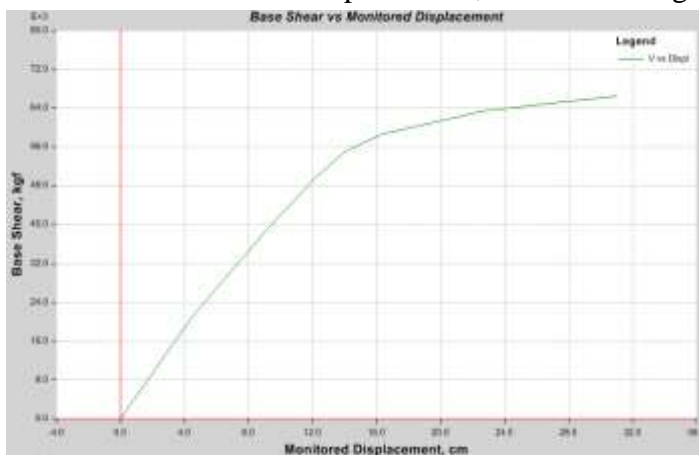


Figure 13 - Structural capacity curve

The target displacement is also calculated according to publication 360 as follows. It should be noted that the values of C1 and C2 are approximately equal to 1 and the coefficient C0 is also calculated according to publication 360 as 1.2.

$$\delta_t = C_0 C_1 C_2 S_a \frac{T_e^2}{4\pi^2} g = 1.2 \times 1 \times 1 \times 0.8 \times \frac{1^2}{4\pi^2} \times 1000 = 24 \text{ cm}$$

By checking the results of the nonlinear analysis, it is determined that in the sixth step of the analysis, the structure has reached the target displacement, therefore, we check the state of the structure in the sixth step (Figure 14).

Figure 14 - Structure condition at target displacement As shown in Figure 14, most of the beams of the structure are located in the LS range and one of the beams of the first floor is located in the CP range. It is also observed that the columns of the structure are located in the LS range. In order to improve the performance level of the base structure, we use divergent steel braces. Therefore, in this stage, we install the braces in the middle span. The brace cross-section is a box type with dimensions of 15 cm. However, in order to find the optimal geometry, four different cases have been considered, the difference of these structures is in the length of the connecting beam. Therefore, the length of the connecting beam in four separate cases is considered to be 1.7, 2.5, 3 and 3.5 meters, and based on that, the names of the models are 2D-B15-E1.7, 2D-B15-E2.5, 2D-B15-E3 and 2D-B15-E3.5, respectively.

2 -1-1-1-3D-B15-E1.7 Model

The length of the connecting beam in this model is considered to be 1.7 meters. The geometry of this model can be seen in Figure 15. The capacity curve of the structure for this model is shown in Figure 16. It can be seen that the maximum displacement tolerated by the structure has decreased. But the important issue is the state of the structure at the target displacement. Because in this case, due to the increase in the stiffness of the structure, the effective period of the structure is reduced to 0.58 and subsequently the target displacement is reduced sharply and reaches 8.5 cm. By checking the results of the nonlinear solution, it is clear that the structure reaches the target displacement in the fourth step of the analysis. Therefore, the state of the structure must be controlled in step 4 of the pushover analysis (according to Figure 17). By checking the state of the structure in the target displacement, it is observed that almost all the beams and columns remain in the elastic state except for the connection beams and its side beams that have entered the LS and CP areas. Therefore, the state of this structure is acceptable if the connection beam and its side beams are also strengthened. In addition, the amount of shear force in the members is also controlled as a force. In Figure 17, the amount of shear forces created in the members of the structure in the target displacement is shown. As can be seen, the shear force in the connection beam is about 32 tons, which, according to the initial design, the structural beams are capable of withstanding this force.

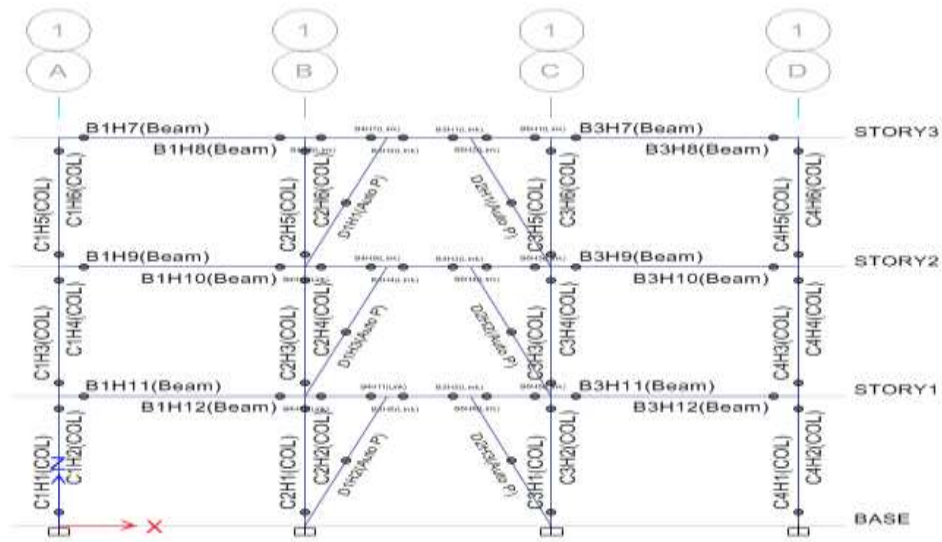


Figure 15 - Structural geometry and joint locations in the 2D-B15-E1.7 model



Figure 16 - Structural capacity curve in the 2D-B15-E1.7 model

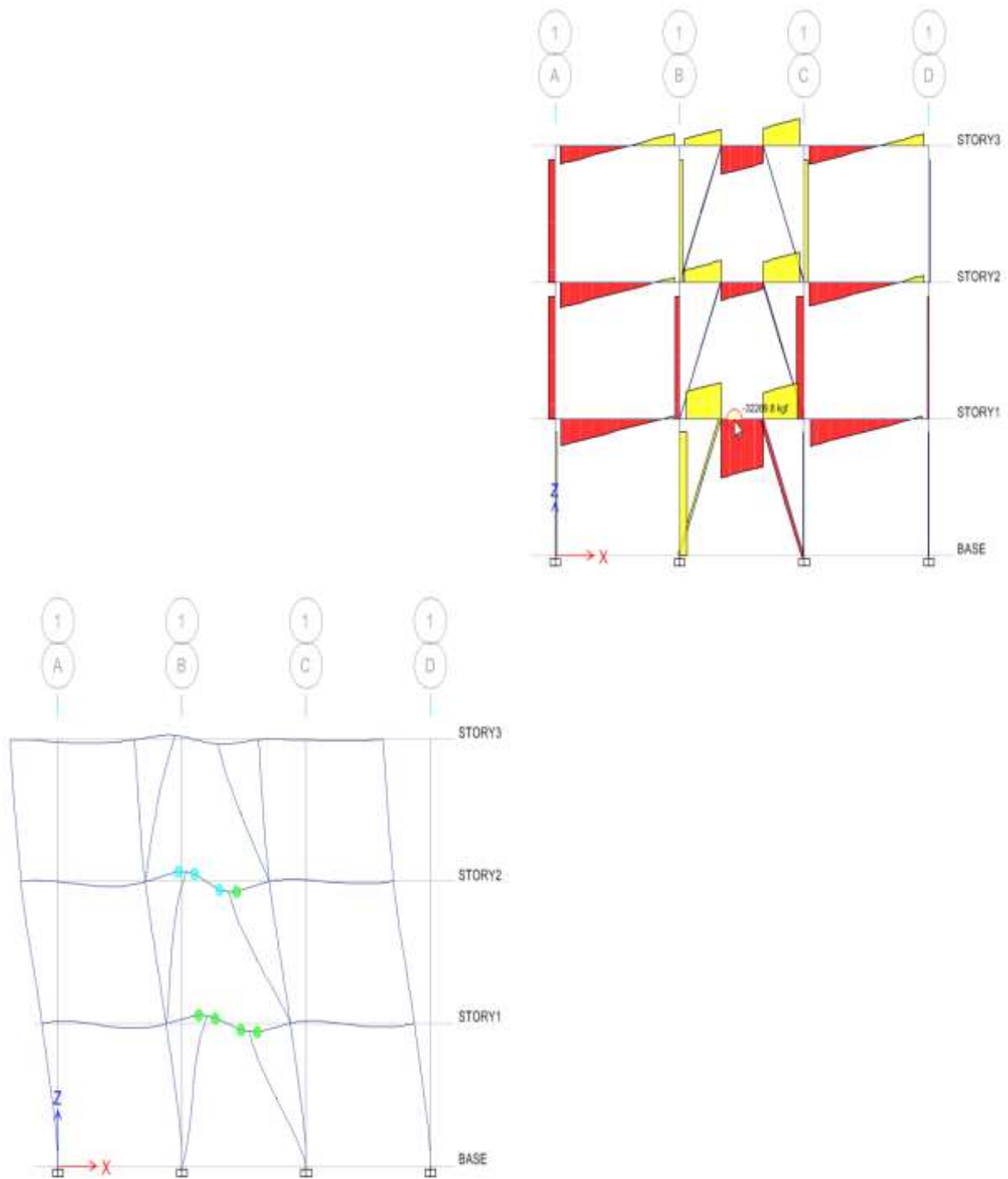


Figure 17- Structure condition and shear force at target displacement

-2-1-1-3Model 2D-B15-E2.5

The length of the link beam in this model is considered to be 2.5 meters. The capacity curve of the structure for this model is shown in Figure 18. In this case, due to the increase in the stiffness of the structure, the effective period of the structure is reduced to 0.71 and subsequently the target displacement is also reduced and reaches 13 centimeters. By controlling the results of the nonlinear solution, it is clear that the structure reaches the target displacement

in the fifth step of the analysis. Therefore, the state of the structure must be controlled in step 5 of the push-pull analysis. By controlling the state of the structure at the target displacement, it is observed that almost all beams and columns remain in the elastic state except for the link beams and their side beams that have entered the LS and CP zones. Therefore, the state of this structure is acceptable if the link beam and its side beams are also strengthened. In addition, the amount of shear force in the members is also controlled in terms of force. As the results show, the amount of shear force in the connection beam is about 32 tons, which according to the initial design, the structural beams are able to withstand this force. However, in the side beams, the shear force has reached about 40 tons. Therefore, the side beams should be slightly strengthened in terms of shear as well.



Figure 18- Structure capacity curve in 2D-B15-E2.5 model

2 -3-1-1-3D-B15-E3 model

The length of the link beam in this model is considered to be 3 meters. In this case, due to the increase in the stiffness of the structure, the effective period of the structure is reduced to 0.79 and subsequently the target displacement is also reduced and reaches 17 cm. By controlling the results of the nonlinear solution, it is clear that the structure reaches the target displacement in the fifth step of the analysis. Therefore, the state of the structure must be controlled in step 5 of the pushover analysis. By controlling the state of the structure in the target displacement, it is observed that almost all beams and columns remain in the elastic state except for the link beams and their side beams that have entered the LS and CP areas. Therefore, the state of this structure is acceptable if the link beam and its side beams are also strengthened. In addition, the amount of shear force in the members is also controlled as a force. As the results show, the amount of shear force in the connecting beam is about 20 tons, which according to the initial design, the structural beams are able to withstand this force. However, in the side beams, the shear force has reached about 36 tons. Therefore, the side beams should also be slightly strengthened in terms of shear.

2 -4-1-1-3D-B15-E3.5 Model

The length of the connecting beam in this model is considered to be 3.5 meters. The capacity curve of the structure for this model is shown in Figure 19. In this case, due to the increase in the stiffness of the structure, the effective period of the structure is reduced to 0.85 and subsequently the target displacement is also reduced and reaches 21 centimeters. By controlling the results of the nonlinear solution, it is clear that the structure reaches the target displacement in the sixth step of the analysis. Therefore, the state of the structure must be controlled in step 6 of the push-pull analysis. By controlling the state of the structure in the target displacement, it is observed that almost all beams and columns remain in the elastic state except for the connection beams and its side beams that have entered the LS and CP zones. Therefore, the state of this structure is acceptable if the connection beam and its side beams are also strengthened. In addition, the amount of shear force in the members is also controlled in terms of force. As the results show, the amount of shear force in the connection beam is about 18 tons, which according to the initial design, the beams of the structure are able to withstand this force. However, in the side beams, the shear force has reached about 56 tons. Therefore, the side beams must be strengthened in terms of shear.



Figure 19- Structural capacity curve in the 2D-B15-E3.5 model

-2-1-3Second case

As mentioned at the beginning, the second case, the base structure is considered in such a way that it has a completely unacceptable performance in the design earthquake and reaches the destruction level. The geometry and shape of the frame in this case is the same as the three-span, three-story frame in Figure 8, with the difference that the characteristics of its element sections have changed in a way that has caused weakness in the structure.

The cross-section of the beams of all floors is considered to be square with dimensions of 40 cm and the upper and lower reinforcements of the section are equal to $3\phi 20$. Also, the dimensions of all columns of the floor are considered to be 40 cm. It is necessary to explain that the longitudinal reinforcements of the column sections are $\phi 25$ and its transverse reinforcements are $\phi 10@125$ mm. According to the above explanations, the characteristics of the bending plastic joint of the beams have been defined. Also, the columns of the structure are defined using the Fiber-M2-M3 element. It should be noted that in this case, due to the

possibility of plastic hinge formation in the structure under the effect of gravity loads, in the beams, in addition to the two ends, a plastic hinge is also defined in the middle of the spans, as shown in Figure 31.

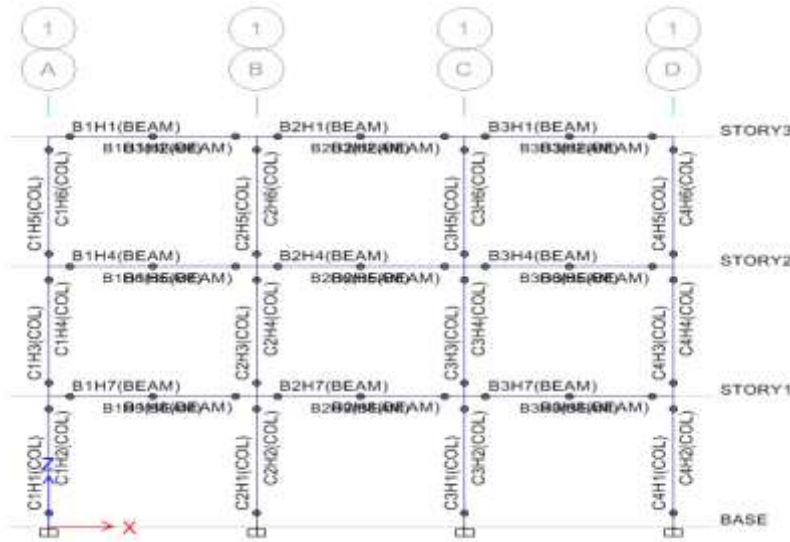


Figure 20 - Location of plastic hinges in structural members

After defining the nonlinear behavior of the structure, gravity loads are first applied to the structure, followed by incremental lateral loads. According to the new edition of the 360 publication, the lateral load distribution used in nonlinear static analysis is considered to be proportional to the first mode of the structure. The capacity curve of the structure, which shows the base shear versus roof displacement, is shown in Figure 21.

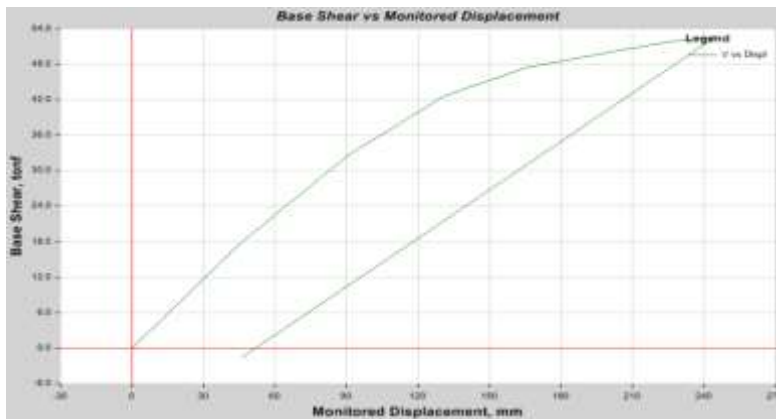


Figure 21 - Structural capacity curve

The target displacement is also calculated according to publication 360 as follows. It should be noted that the values of C_1 and C_2 are approximately equal to 1 and the coefficient C_0 is also calculated according to publication 360 as 1.2.

$$\delta_t = C_0 C_1 C_2 S_a \frac{T_e^2}{4\pi^2} g = 1.2 \times 1 \times 1 \times 0.8 \times \frac{1.1^2}{4\pi^2} \times 1000 = 33 \text{ cm}$$

By checking the results of the nonlinear analysis, it is determined that the structure will collapse before reaching the target displacement (Figure 22).

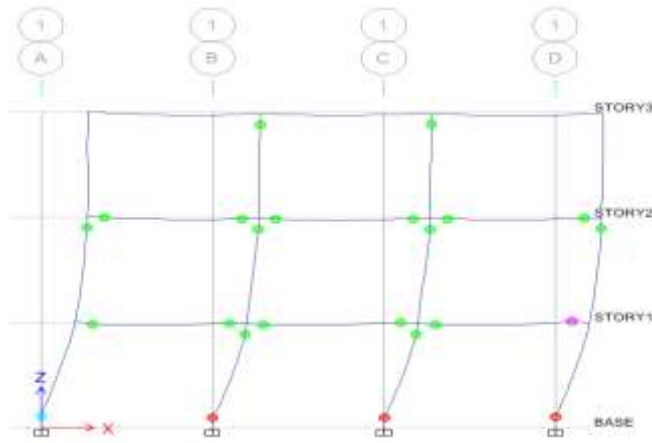


Figure 22 - Collapse of the structure

In order to strengthen the base structure, we use divergent steel braces. Therefore, at this stage, we install the braces in the middle span. The brace cross-section is a box type with dimensions of 15 cm.

However, in order to find the optimal geometry, three different cases have been considered, the difference between these structures is in the length of the connecting beam. Therefore, the length of the connecting beam in three separate cases is considered to be 1.7, 2.5 and 3 meters, and based on that, the names of the models are 2D-B15-E1.7, 2D-B15-E2.5 and 2D-B15-E3, respectively.

2 -1-2-1-3D-B15-E1.7 model

The length of the connecting beam in this model is considered to be 1.7 meters. The geometry of this model can be seen in Figure 23.

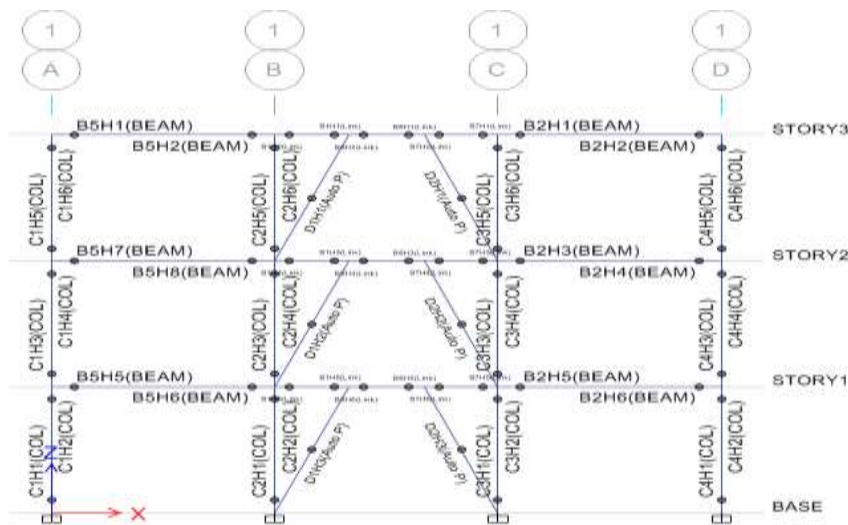


Figure 23 - Structure geometry and joint locations in the 2D-B15-E1.7 model

The capacity curve of the structure for this model is shown in Figure 24. It can be seen that the maximum displacement tolerated by the structure has decreased. However, the important issue is the state of the structure at the target displacement. Because in this case, due to the increase in the stiffness of the structure, the effective period of the structure is reduced to 0.62 and subsequently the target displacement is reduced sharply and reaches 10.5 cm. By controlling the results of the nonlinear solution, it is clear that the structure reaches the target displacement in the sixth step of the analysis. Therefore, the state of the structure must be controlled in step 6 of the pushover analysis (according to Figure 25). By controlling the state of the structure at the target displacement, it is observed that almost all beams and columns have remained in the elastic state except for the connection beams and its side beams, which have undergone very high rotations and have reached the point of collapse. In addition, the amount of shear force in the members is also controlled as a force. In Figure 25, the amount of shear forces generated in the structural members at the target displacement is shown. As can be seen, the amount of shear force in the connecting beam is about 46 tons and requires strengthening.

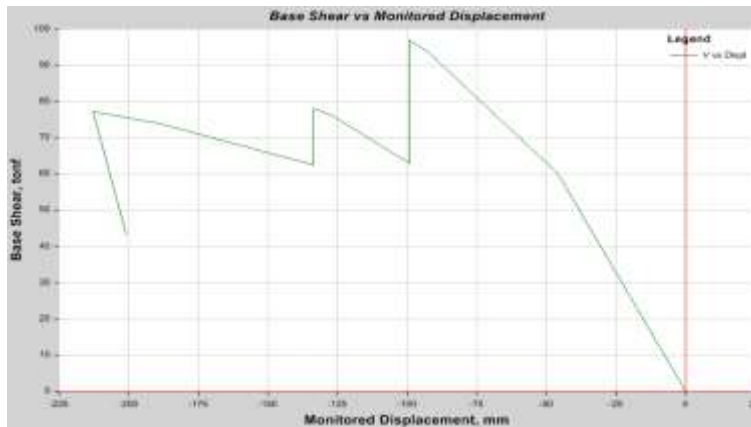


Figure 24- Structural capacity curve in the 2D-B15-E1.7 model

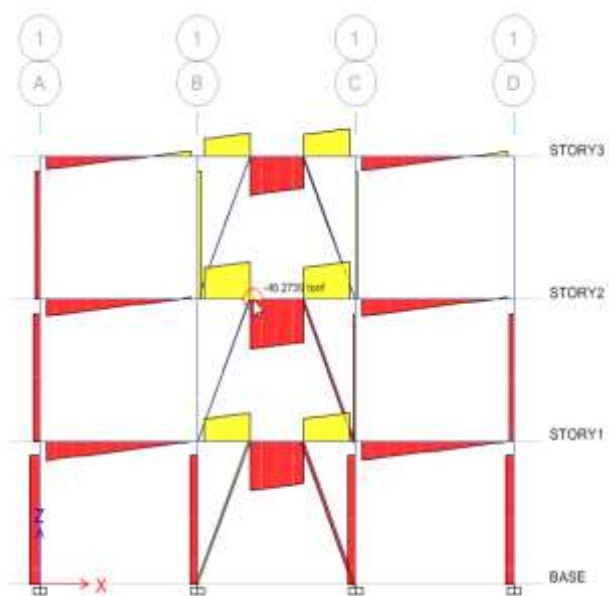
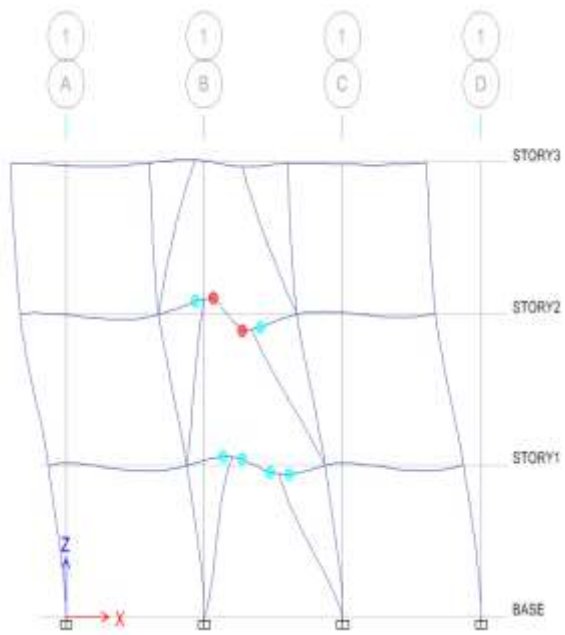


Figure 25- Structural condition and member shear force at target displacement

2 -2-2-1-3D-B15-E2.5 model

The length of the link beam in this model is considered to be 2.5 meters. The capacity curve of the structure for this model is shown in Figure 26. It can be seen that in this case, due to the increase in structural stiffness, the effective period of the structure is reduced to 0.78 and subsequently the target displacement is greatly reduced and reaches 12 centimeters. By controlling the results of the nonlinear solution, it is clear that the structure reaches the target displacement in the third step of the analysis. Therefore, the state of the structure must be controlled in step 3 of the pushover analysis. By controlling the state of the structure at the target displacement, it is observed that all columns remain in an elastic state, but all beams, including the link beams and their side beams, have undergone very high rotations and have reached the point of collapse. In addition, the amount of shear force in the members is also controlled in a force-wise manner. As the results show, the amount of shear force in the connection beam is about 33 tons and its resistance is sufficient and does not require reinforcement.



Figure 26- Structural capacity curve in 2D-B15-E2.5 model

2 -3-2-1-3D-B15-E3 model

The length of the connecting beam in this model is considered to be 3 meters. The structural capacity curve for this model is shown in Figure 27. It is observed that the maximum displacement tolerated by the structure has decreased. However, in this case, due to the increase in the stiffness of the structure, the effective period of the structure has decreased to 0.87 and subsequently the target displacement has decreased sharply and reached 13.5 cm. By controlling the results of the nonlinear solution, it is clear that the structure reaches the target

displacement in the fifth step of the analysis. Therefore, the state of the structure must be controlled in step 5 of the pushover analysis. By controlling the state of the structure in the target displacement, it is observed that in this case, a hinge is formed at the foot of the columns but its rotation is limited to the life safety limit LS. But the connection beams still have the highest rotation and it is observed that they need local strengthening. In addition, the amount of shear force in the members is also controlled in terms of force. As the results show, the amount of shear force in the connection beam is small, but in its side beams, the shear force is about 46 tons and needs strengthening.

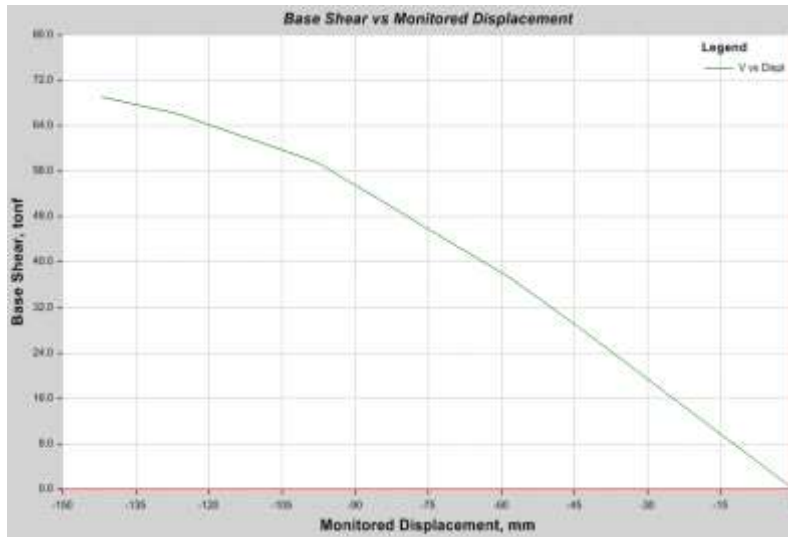


Figure 27- Structural capacity curve in the 2D-B15-E3 model
-2-3Results from the two studied cases

By examining the results, it can be said that adding divergent braces to concrete flexural frames can be very effective in structures whose performance level is very difficult (destructive structures). It can be seen that in the structures studied based on the second scenario, the performance level of the structure before and after strengthening is very different, and if we strengthen the connecting beams locally, a destructive structure can be upgraded to the IO and LS performance levels. On the other hand, the most optimal geometry in this study is the case where the length of the connecting beam is equal to the length of its side beams, in other words, the location of the steel braces is at one third of the beam span.

-4Performance of the optimized reinforced concrete frame with divergent Sherwin braces and reinforcement of the connecting beam

According to the studies carried out in the previous sections, in this section, the 2D-B15-E1.7 model, which was related to the second case, was selected as the most optimal model and further studies were carried out on it. In this section, assuming local reinforcement of the connecting beam, we investigate the seismic behavior of this frame.

In the modeling, it is assumed that the connecting beam is reinforced using one of the strengthening methods and its yield moment is 30 Ton.m and its shear capacity is 53 tons. With these assumptions, the capacity curve of the structure is obtained as shown in Figure 28. In this structure, due to the increase in the stiffness of the structure, the effective period of the structure is reduced to 0.62 and subsequently the target displacement is greatly reduced and reaches 10.5

cm. By checking the results of the nonlinear solution, it is determined that the structure reaches the target displacement between the third and fourth steps of the analysis. Therefore, the state of the structure in steps 3 and 4 of the pushover analysis (according to Figures 29 and 30) should be checked and its average should be used as the criterion.



Figure 28 - Capacity curve of reinforced sample

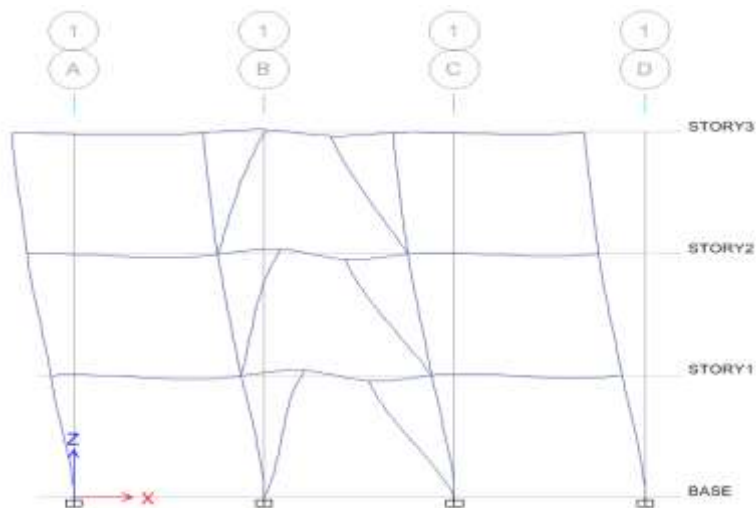


Figure 29 - Structural condition in step 3 of the analysis

By checking the structural condition in step 3, it is determined that the entire structure is elastic and in step 4 the structure is within the LS range, one member has also reached the CP limit. Therefore, on average, it can be said that the entire structure has provided the life safety performance level.

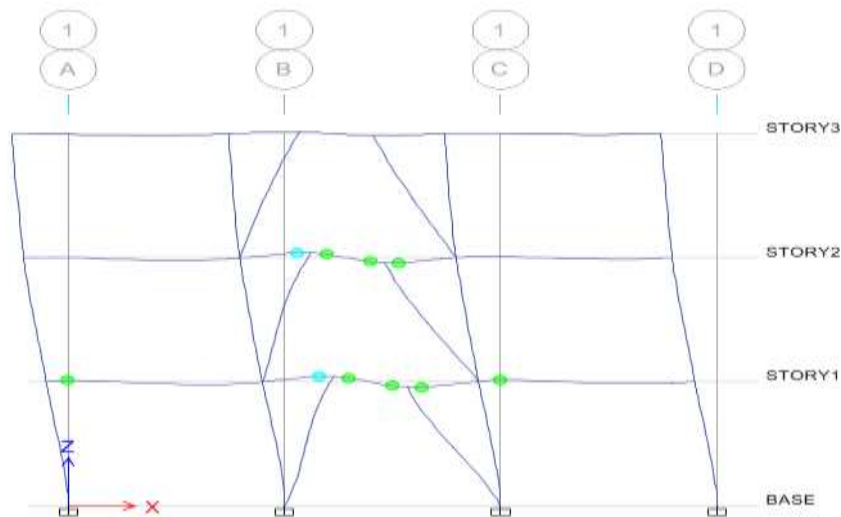


Figure 30 - Structure condition in step 4 of analysis

In addition, the amount of shear force in the members is also controlled in the form of force. In Figure 31, the amount of shear forces created in the structural members in step 4 is shown. As can be seen, the amount of shear force in the connection beam is about 54 tons, and considering that the average of steps 3 and 4 is the criterion, it can be said that the shear capacity of the beam is responsive to the created shear.

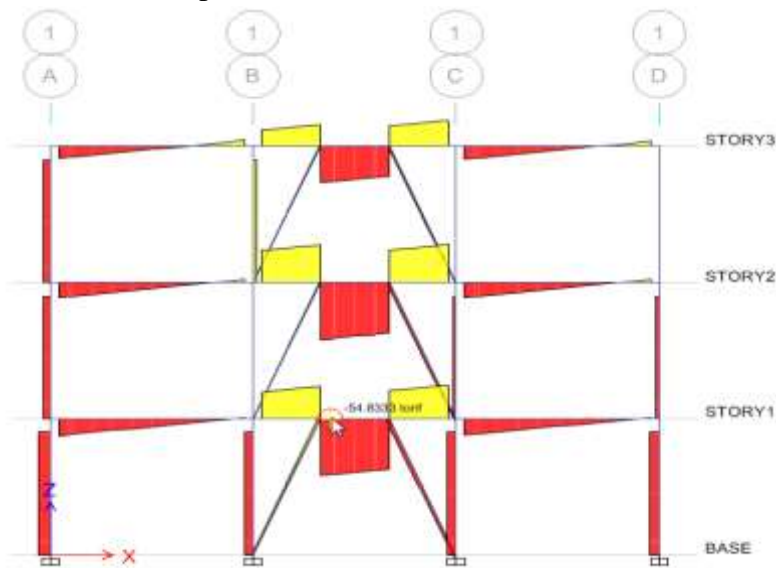


Figure 31- Shear force in members at step 4

-1-4System ductility

In order to examine the ductility of the system, it is necessary to first convert the capacity curve into a bilinear form. It should be noted that in bilinearizing the curve, due to the special shape of the curve of this structure, the criterion of 60% of the effective base shear cannot be observed, and therefore, according to existing references, the curve is bilinearized with the initial stiffness and the area under the bilinear curve is also equal to the area under the capacity curve. In Figure 32, the bilinear curve of the structure is shown.

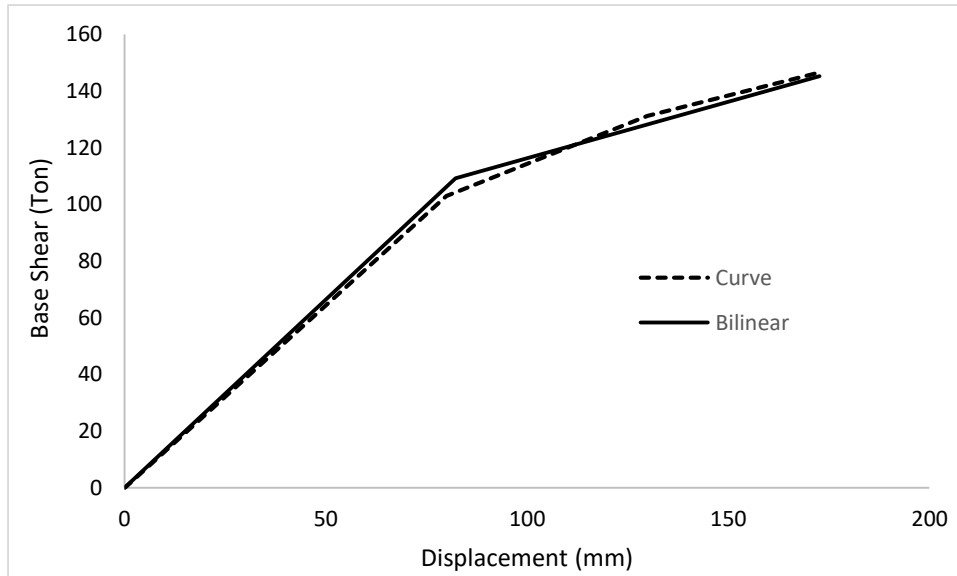


Figure 32 - Bilinearization of the capacity curve

The ductility requirement is also equal to the target displacement to the effective yield displacement in the bilinear curve. The target displacement in this structure is equal to 10.5 cm and the effective yield displacement in the bilinear curve is equal to 8.2 cm, therefore, the system ductility requirement is equal to 1.28. The system ductility capacity is equal to the maximum displacement that can be tolerated by the structure to the effective yield displacement in the bilinear curve, which, according to the above curve, results in the system ductility capacity equal to 1.2. Thus, according to the principle of equal displacements of linear and nonlinear systems, the behavior coefficient corresponding to the ductility R_μ is equal to 1.2.

If we calculate the behavior coefficient corresponding to the ductility R_μ in all the structures examined in this study, the average value is 2.45. Therefore, the average value of this parameter is considered equal to this value and we have:

$$R_\mu = 2.45$$

-2-4 System additional resistance coefficient

The system additional resistance coefficient Ω_0 is equal to the base shear created in the structure when the effective base shear mechanism of the structure is formed in the bilinear curve. In this structure, the value of the additional resistance coefficient is equal to about 1.5. By calculating the value of the additional resistance coefficient Ω_0 in all the investigated structures and averaging it, the average value of this parameter is obtained equal to 2.5 and we have:

$$\Omega_0 = 2.5$$

-3-4 System behavior coefficient

The system behavior coefficient at the allowable stress level (based on the third edition of Regulation 2800) is equal to the behavior coefficient corresponding to the ductility of the system multiplied by its additional resistance coefficient in the allowable stress method coefficient, which in this structure is obtained as 8.58 according to the calculations below.

$$R = R_\mu \times \Omega_0 \times Y = 2.45 \times 2.5 \times 1.4 = 8.58$$

4-4- Failure modes

As observed in the previous sections, the failure modes of flexural frames are mainly of the widespread type and occur in all structural members. In these structures, plastic hinges are usually formed at the ends of the beams and at the base of the columns, which makes it very difficult to strengthen the structure after an earthquake. However, by adding divergent steel braces to concrete flexural frames, all plastic deformations are concentrated at the connection beam location, and after an earthquake, it is sufficient to locally strengthen only the connection beam.

5- Conclusion

The results extracted from this research are as follows:

- 1- Adding divergent metal braces to concrete frames can improve the performance level of the structure to several levels.
- 2- Adding divergent metal braces to concrete frames that have a very low performance level (destructive) will have the greatest results.
- 3- Adding divergent metal braces to concrete frames causes plastic deformations to concentrate in the connection beam, and therefore the connection beam must also be locally strengthened.

The most optimal arrangement of divergent braces in concrete beams (in this study) is such that the intersection of the braces should divide the concrete beam into three equal parts.

The ductility of concrete flexural frames strengthened with divergent metal braces is about 2.5.

The behavior coefficient corresponding to the ductility of concrete flexural frames strengthened with divergent metal braces is about 2.5.

The additional resistance coefficient of concrete flexural frames strengthened with divergent metal braces is about 2.5.

The behavior coefficient of concrete flexural frames strengthened with divergent metal braces is about 5.8.

References

- [1] Priestley, M.J.N., Calvi, G.M., Kowalsky, M.J., "Displacement-Based Seismic Design of Structures", IUSS Press, Italy, 2007.
- [2] Yaseen, Pari. "Analytical Study on Seismic Strengthening of Existing Reinforced Concrete Buildings by Implementation of Energy Absorbers." Master's thesis, Eastern Mediterranean University (EMU)-Doğu Akdeniz Üniversitesi (DAÜ), 2022.
- [3] Shiri, Yousef, Jafar Keyvani, and Seyed Hossein Hoseini Lavassani. "Analytical Solution of the Closed-Form Equations Governing the Hybrid Performance of a Tuned Liquid Column Gas Damper Equipped With a Variable Orifice." *Journal of Rehabilitation in Civil Engineering* 13, no. 3 (2024): 104-128.
- [4] Alshimmeri, Ahmad Jabbar Hussain, Denise-Penelope N. Kontoni, and Ali Ghamari. "Improving the seismic performance of reinforced concrete frames using an innovative metallic-shear damper." *Computers and Concrete* 28, no. 3 (2021): 275.
- [5] Zakian, Pooya, and Ali Kaveh. "Multi-objective seismic design optimization of structures: a review." *Archives of Computational Methods in Engineering* 31, no. 2 (2024): 579-594.
- [6] FEMA-356, "Prestandard and Commentary for the Seismic Rehabilitation of Buildings" American Society of Civil Engineers, Federal Emergency Management Agency, Washington, D.C., (2000).
- [7] Sugano, S. and Fujimura, M., "Seismic strengthening of existing reinforced concrete building" *proc. Of the seventh world conference on earth. eng , part 1, vol14, Turkey-1980*, pp. 449-459.
- [8] Ghobarah ,A. and Abou Elfath, H., "Rehabilitation of A Reinforced Concrete Frame Using Eccentric Steel Bracing", *Engineering Structures*, Issue7, 2001, vol23, pp. 745-755.
- [9] Badoux ,M. and Jirsa, J. O., "Steel Bracing of RC Frame For Seismic Retrofitting", *Journal of Structures Engineering*, 1990, No.1, vol.116, pp. 55-74.
- [10] Mohsen Gerami et al., "Reinforcing Reinforced Concrete Frames with Steel Braces," *Proceedings of the 14th National Conference of Civil Engineering Students*, 2008.
- [11] Maheri ,M. and Sahebi,A., "Experimental Investigation of Steel-Braced Reinforced Concrete Frames", *proceeding of Second International Conference on Seismology and Earthquake Engineering*, Tehran, Islamic Republic of Iran, 1995
- [12] Khatib ,I.F., Mahin, S.A., and Pister, K.S., "Seismic behavior of concentrically braced steel frames", *Report UCB/EERC-88/01, Earthquake Engineering Research Center, University of California, Berkeley, Calif*, 1988.
- [13] Freeman, A , " Review of Development of the Capacity Spectrum Method", *ISET journal of Earthquake Technology*, Vol. 41, No.1, pp. 1-13., (2004).
- [14] Yuan Lin, Yu., And Chun Chang, Kuo., And Hao Tsai, Meng., "Displacement – Based Seismic Design For Building", *Jornal of Chinese Institute Of Engineers*, Vol. 25, No.1, pp. 89-98., (2002).

- [15] Jindani, Mehboob H. "Displacement Based Design Of Wall-Frame and Shear Wall Buildings." PhD diss., Institute of Technology, 2014.
- [16] Durucan, Cengizhan, and Murat Dicleli. "Analytical study on seismic retrofitting of reinforced concrete buildings using steel braces with shear link." *Engineering Structures* 32, no. 10 (2010): 2995-3010.
- [17] Keivan, Arshia, and Yunfeng Zhang. "Nonlinear seismic performance of Y-type self-centering steel eccentrically braced frame buildings." *Engineering Structures* 179 (2019): 448-459.
- [18] Tabeshpour, Mohammad Reza., "Application of incremental load (pushover analysis) and capacity spectrum in seismic retrofitting of existing structures", *Proceedings of the First International Conference on Seismic Retrofitting*, Tehran, Iran, 25-26 May, (2006).